CHAPTER 2

HYDRODYNAMIC LUBRICATION OF POROUS BEARINGS

In the following sections we study the hydro-
dynamic lubrication of a porous composite slider, a porous
exponential slider and of a squeeze film trapped between
a curved plate and a flat plate.

2.1   A COMPOSITE SLIDER BEARING[*]

The slider bearing is the simplest and is
encountered most often. It is because the expression for
film thickness is simple and the boundary conditions are
less complicated. In such bearings the film is non-diverging
and continuous and so, the problem of negative pressure does
not arise. Such bearings are designed to support axial
loads. They are applied in hydroelectric generators, steam
and gas turbines and in other equipments.

The analysis of hydrodynamic lubrication of a
composite slider bearing is a classical one [38]. The
hydromagnetic composite slider bearing with inclined and
flat parts in the presence of a transverse magnetic field
was studied by Prakash [39]. Later, Agrawal [40]
investigated the above configuration taking into account

[*]Accepted for publication in Jap. J. of Appl. Phys.

the electrical conductivity of both the bearing and the
slider. He approximated the velocity profile of the fluid
under the inclined part by the superposition of the velocity
profiles for rectangular channel flow and couetee flow.
Both the above investigators assumed the stator and
slider to be impermeable.

In this section we consider the lubrication
of a non-magnetic porous composite slider bearing without
using the approximation of Agrawal [40]. We consider
the velocity profiles under the inclined part and the
flat part separately as was done by Hughes [41].

2.1.1 Mathematical formulation

The configuration of the bearing which is
infinite in the z-direction is shown in Fig. 4. The slider
consists of a plate inclined to the stator with its
x-length A and another plate of length A_1 parallel to
the stator, both being rigidly connected. It moves
parallel to itself with a uniform velocity U. The stator
has a porous facing of thickness H which is backed by
a solid wall. Following the assumptions of hydrodynamic
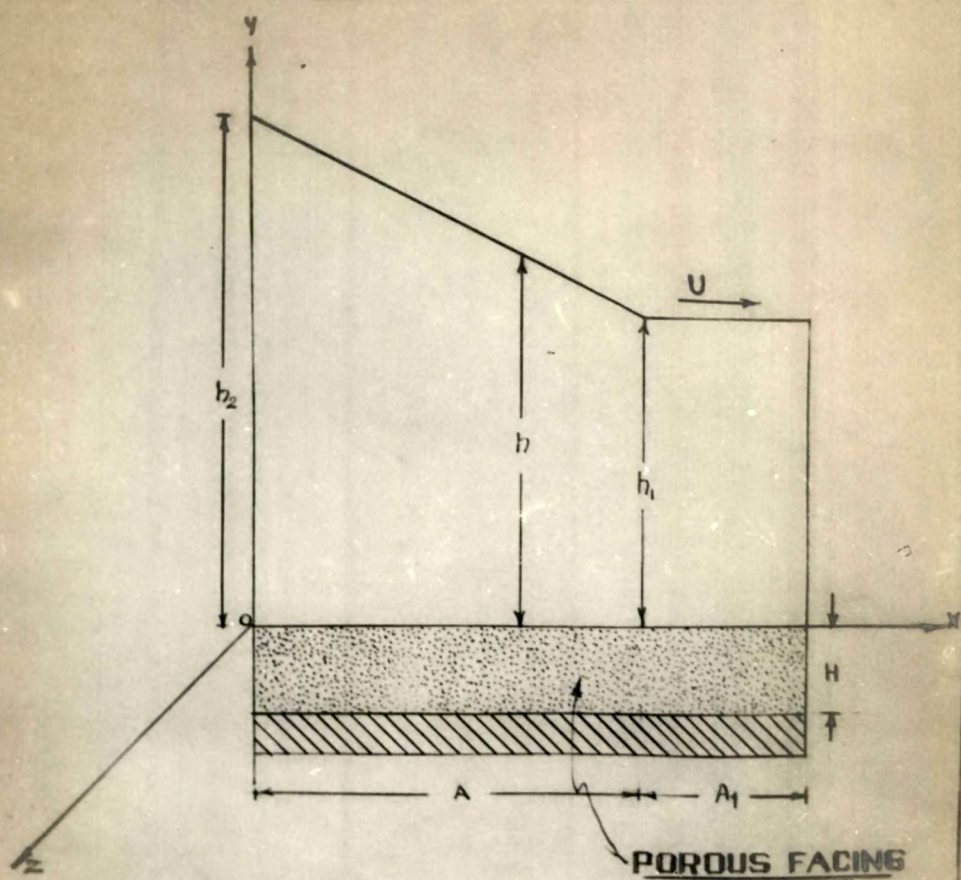lubrication of 1.2, the governing equation for both the

FIG. 4. POROUS COMPOSITE SLIDER BEARING.

regions, under the inclined plate as well as parallel plate, is

$$\frac{d}{dx}\left[(h^3 + 12kH)\frac{dp}{dx}\right] = 6\mu U\frac{dh}{dx} \tag{1}$$

for appropriate values of the film thickness h. Introducing the dimensionless quantities

$$\bar{x} = \frac{x}{A} \ , \quad \bar{h} = \frac{h}{h_1} \ , \quad \bar{p} = \frac{h_1^2 p}{\mu U A} \ , \quad \alpha^3 = 12\psi = 12\frac{kH}{h_1^3} \tag{2}$$

into equation (1) and integrating it once with respect to x, we have

$$\frac{d\bar{p}}{d\bar{x}} = 6\ \frac{\bar{h} + Q}{\bar{h}^3 + \alpha^3} \ , \tag{3}$$

where Q is the constant of integration to be determined.

2.1.2 Solutions

The dimensionless pressure $\bar{p}_1$ under the inclined plate is obtained by solving equation (3) after substituting

$$\bar{h} = a - (a - 1)\ \bar{x} \ , \tag{4}$$

where $a = h_2/h_1$, and using the boundary condition

$$\bar{p}_1 = 0 \quad \text{when} \quad \bar{x} = 0 \tag{5}$$

as

$$\bar{p}_1 = - \frac{1}{a-1} \left[\frac{1}{\alpha} \left\{ L_1 - L + 2\sqrt{3}(T-T_1) \right\} + \frac{Q_1}{\alpha^2} \left\{ L-L_1 + 2\sqrt{3}(T-T_1) \right\} \right] \tag{6}$$

where

$$L = \ln \left[\frac{(\bar{h} + \alpha)^2}{\bar{h}^2 - \alpha\bar{h} + \alpha^2} \right] , \quad T = \tan^{-1}\left(\frac{2\bar{h} - \alpha}{\alpha\sqrt{3}} \right) \left. \vphantom{\frac{(\bar{h}+\alpha)^2}{\bar{h}^2}} \right\} \tag{7}$$

and L_1, L_2 and T_1, T_2 are their values when $\bar{h} = a$ and $\bar{h} = 1$ respectively.

The dimensionless pressure p_2 under the parallel plate is obtained by solving equation (3) after substituting $\bar{h} = 1$ and using the boundary condition

$$\bar{p}_2 = 0 \quad \text{when} \quad \bar{x} = 1 + \bar{A}_1 \,, \tag{8}$$

where

$$\bar{A}_1 = A_1/A \,,$$

as
$$\bar{p}_2 = 6 \frac{(1+Q_2)}{1+\alpha^3} \quad (\bar{x} - 1 - \bar{A}_1) \,. \tag{9}$$

The constants Q_1 and Q_2 are to be determined. Owing to the continuity of the pressures and the flow rates in the x-direction across $\bar{h} = 1$, we have

$$-\frac{1}{a-1} \left[\frac{1}{\alpha} \left\{ L_1 - L_2 + 2\sqrt{3}(T_2 - T_1) \right\} + \frac{Q_1}{\alpha^2} \left\{ L_2 - L_1 + 2\sqrt{3}(T_2 - T_1) \right\} \right]$$

$$= 6 \frac{1 + Q_2}{1 + \alpha^3} \quad (-\bar{A}_1) \tag{10}$$

and

$$Q_1 = Q_2 \tag{11}$$

Equations (10) and (11) yield

$$Q_1 = Q_2 = \frac{(1+\alpha^3)\alpha \left\{ L_1 - L_2 + 2\sqrt{3}(T_2 - T_1) \right\} - 6(a-1)\alpha^2 \bar{A}_1}{(1+\alpha^3) \left\{ L_1 - L_2 + 2\sqrt{3}(T_1 - T_2) \right\} + 6(a-1)\alpha^2 \bar{A}_1} \,. \tag{12}$$

The load capacity W is defined as

$$W = \int_0^B \int_0^A p_1 \, dx \, dz + \int_0^B \int_A^{A+A_1} p_2 \, dx \, dz \, ,$$

where p_1, p_2 are the pressures under the inclined and the parallel plates respectively.

The dimensionless load capacity of the bearing is

$$\bar{W} = \frac{h_1^2 \, W}{\mu U A^2 B} = \frac{1}{(a-1)^2} \left[2 \ln \left(\frac{a^3 + \alpha^3}{1 + \alpha^3} \right) \right.$$

$$+ \frac{(a - Q_1)}{\alpha} \left\{ L_1 - L_2 + 2\sqrt{3} \, (T_2 - T_1) \right\}$$

$$+ \frac{aQ_1}{\alpha^2} \left\{ L_2 - L_1 + 2\sqrt{3} \, (T_2 - T_1) \right\} \right]$$

$$- 3 \, \frac{1 + Q_1}{1 + \alpha^3} \, (2 + \bar{A}_1) \, \bar{A}_1. \tag{13}$$

The frictional drag F exerted by the moving slider is defined as

$$F = \int_0^B \int_0^{A+A_1} \mu \left(\frac{\partial u}{\partial y} \right)_{y=h} dx dz.$$

The dimensionless friction is

$$\bar{F} = \frac{h_1 F}{\mu U A B} = \frac{1}{a-1} \left[\ln\left(\frac{a^3 + \alpha^3}{1 + \alpha^3} \right) - \frac{Q_1}{2\alpha} \left\{ L_1 - L_2 + 2\sqrt{3}(T_2 - T_1) \right\} \right]$$

$$+ \frac{\ln a}{a-1} + \left[3 \frac{1 + Q_1}{1 + \alpha^3} + 1 \right] \bar{A}_1. \qquad (14)$$

The x-coordinate $\bar{\bar{x}}$ of the centre of pressure is given by

$$\bar{\bar{x}} = \frac{1}{W} \left[\int_0^B \int_0^A p_1 x \, dx dz + \int_0^B \int_A^{A+A_1} p_2 x \, dx dz \right],$$

and in dimensionless form it is obtained as

$$\frac{\bar{\bar{x}}}{A} = \frac{1}{2(a-1)^3 \bar{W}} \left[6(1-a) + 2(Q_1 - 2a)\ln\left(\frac{1 + \alpha^3}{a^3 + \alpha^3} \right) \right.$$

$$+ \frac{(a^2 - 2aQ_1)}{\alpha} \left\{ L_1 - L_2 + 2\sqrt{3}(T_2 - T_1) \right\} + \frac{(a^2 Q_1 - \alpha^3)}{\alpha^2}$$

$$\left. \cdot \left\{ L_2 - L_1 + 2\sqrt{3}(T_2 - T_1) \right\} \right] - \frac{1 + Q_1}{1 + \alpha^3} (3 + 3\bar{A}_1 + \bar{A}_1^2) \frac{\bar{A}_1}{\bar{W}} \qquad (15)$$

where Q_1 appearing in equations (13) - (15) is given by (12).

2.1.3 Results and discussion

Setting $\bar{A}_1 = 0$, we obtain the results for an inclined slider bearing in a form equivalent to that of Prakash and Vij [37].

Taking $A = 0$, we have the case of a parallel plate porous slider bearing . It can be seen that in this case the load capacity W becomes zero.

The dimensionless load capacity, centre of pressure and friction are expressed in equation (13) - (15) as functions of $\bar{A}_1$ and ψ . The numerical results for the above characteristics are shown in Tables 1 to 3.

It is seen from Table 1 that, for a given value of a, load capacity $\bar{W}$ decreases when the permeability parameter increases. For values of $\psi > 0.01$, the decrease in load is significant as compared to that of a solid bearing. On the other hand, the load increases with $\bar{A}_1$.

Table 2 shows that the centre of pressure

moves towards the outlet face when $\overline{A}_1$ increases, while it moves towards the middle of the bearing when ψ increases.

It is seen from Table 3 that while the friction increases with $\overline{A}_1$, it decreases when ψ increases.

Thus, it can be seen that the porous composite slider has more load capacity than the corresponding porous inclined slider.

TABLE 1

Values of dimensionless load capacity $\overline{W}$ for various values of ψ and $\overline{A}_1$. a = 2.

$\overline{A}_1$ \ ψ	0.0001	0.0010	0.0100	0.1000	1.0000
0.00	0.159	0.158	0.151	0.109	0.032
0.05	0.190	0.189	0.181	0.128	0.037
0.10	0.219	0.218	0.208	0.147	0.041
0.15	0.246	0.245	0.234	0.164	0.046
0.20	0.272	0.270	0.258	0.182	0.051

TABLE 2

Values of dimensionless centre of pressure $\frac{\equiv}{\overline{X}}{A}$ for various values of ψ and $\overline{A}_1$. a = 2.

$\overline{A}_1$ \ ψ	0.0001	0.0010	0.0100	0.1000	1.0000
0.00	0.569	0.568	0.567	0.548	0.514
0.05	0.602	0.602	0.599	0.578	0.541
0.10	0.634	0.634	0.630	0.609	0.569
0.15	0.665	0.664	0.661	0.638	0.596
0.20	0.693	0.692	0.689	0.665	0.622

TABLE 3

Values of dimensionless friction $\overline{F}$ for various values of ψ and $\overline{A}_1$. a = 2.

$\overline{A}_1$ \ ψ	0.0001	0.0010	0.0100	0.1000	1.0000
0.00	0.773	0.772	0.769	0.747	0.709
0.05	0.837	0.837	0.832	0.807	0.761
0.10	0.899	0.898	0.894	0.864	0.813
0.15	0.958	0.958	0.953	0.921	0.865
0.20	1.016	1.015	1.010	0.977	0.917

2.2   AN EXPONENTIAL SLIDER BEARING

The idea behind the tilting pad thrust bearings was to put a pivot on a flat sector shaped pad just behind the mid point. The classical theory assumed the pad stayed flat and so the analysis considered a wedge. In practice the pad is found to bend elastically and distorted by thermal effects. This results in the shape of the bearing far from a straight wedge. Cameron [42] considered the exponential film to be nearest the true shape. Moreover, considerable simplification was introduced by expressing the film thickness by an exponential form and the performance of thrust bearings depended mainly on the maximum and minimum film thicknesses and much less on the actual shape between inlet and outlet faces [38]. While the above investigations were on solid surfaces, in this section we consider the lubrication of a porous exponential slider.

2.2.1 Mathematical formulation

The configuration consists of a slider, infinite along the z-direction and moving with a uniform velocity U in the x-direction, and stator having a

porous facing of thickness H (Fig. 5). The fluid film
has a thickness h given by

$$h = h_2 \, e^{-\frac{x}{A} \ln a} \qquad\qquad (16)$$

where

$$0 \leq x \leq A \quad \text{and} \quad a = h_2/h_1. \qquad\qquad (17)$$

In dimensionless form it is

$$\bar{h} = a \, e^{-\bar{x} \ln a} \qquad\qquad (18)$$

where

$$\bar{h} = \frac{h}{h_1} \quad \text{and} \quad \bar{x} = \frac{x}{A}. \qquad\qquad (19)$$

Following the assumptions of hydrodynamic
lubrication of 1.2, the governing equation for film
pressure is

$$\frac{d}{dx} \left[(h^3 + 12kH) \frac{dp}{dx} \right] = 6 \, \mu \, U \, \frac{dh}{dx} \qquad\qquad (20)$$

which, in dimensionless form, may be written as

$$\frac{d}{d\bar{x}} \left[(\bar{h}^3 + \alpha^3) \frac{d\bar{p}}{d\bar{x}} \right] = 6 \, \frac{d\bar{h}}{d\bar{x}}. \qquad\qquad (21)$$
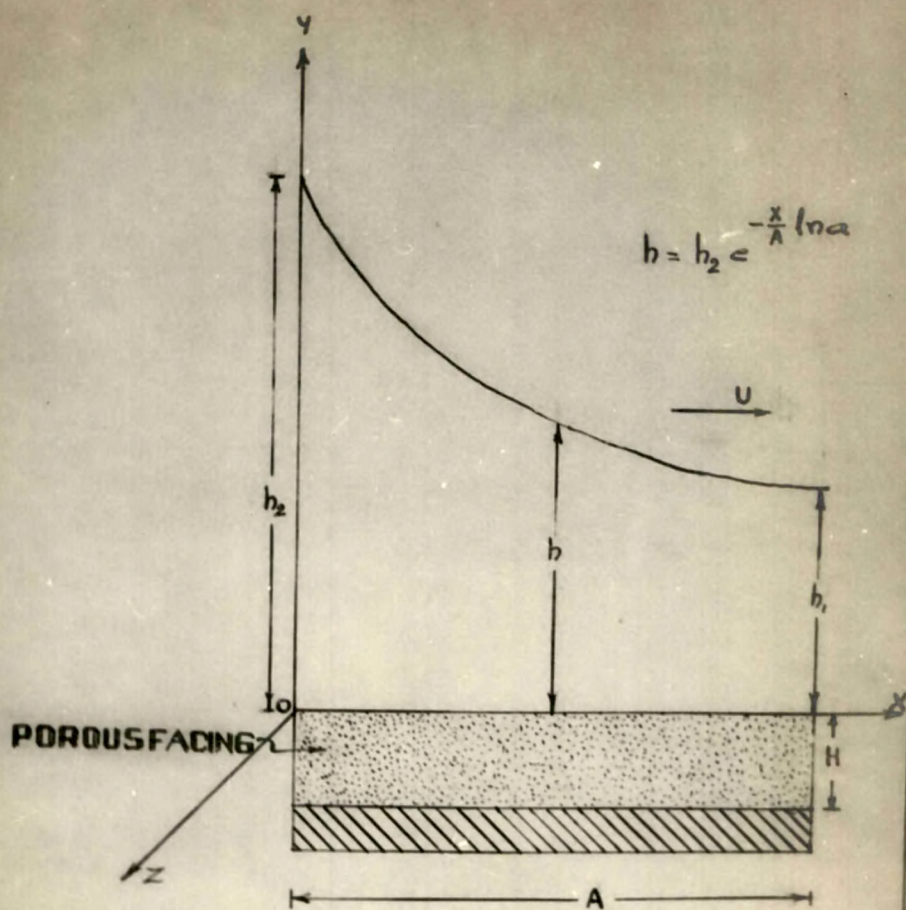
$$h = h_2 \, e^{-\frac{x}{A} \ln a}$$

FIG. 5. POROUS EXPONENTIAL SLIDER BEARING.

Integrating equation (21) with the condition

$$\frac{d\bar{p}}{d\bar{x}} = 0 \quad \text{when} \quad \bar{h} = \bar{h}_0 , \qquad (22)$$

where $\bar{h}_0$ is the film thickness at the point of maximum pressure, we have

$$\frac{d\bar{p}}{d\bar{x}} = 6 \left(\frac{\bar{h} - \bar{h}_0}{\bar{h}^3 + \alpha^3}\right) \qquad (23)$$

which in view of (18) takes the form

$$\frac{d\bar{p}}{d\bar{h}} = \frac{6(\bar{h}_0 - \bar{h})}{\bar{h}(\bar{h}^3 + \alpha^3)\ln a} \qquad (24)$$

2.2.2 Solutions

Solving equation (24) under the boundary conditions

$$\bar{p}(\bar{h} = 1) = \bar{p}(\bar{h} = a) = 0, \qquad (25)$$

the dimensionless pressure distribution is obtained as

$$\bar{p} = \frac{h_1^2 \, p}{\mu \overline{U} A} = \frac{1}{\alpha^2 \ln a} \left[\frac{L_1 - L_2 + 2\sqrt{3}\,(T_1 - T_2)}{\ln \left\{ \frac{a^3(1 + \alpha^3)}{a^3 + \alpha^3} \right\}} \right.$$

$$\left. \cdot \ln \left\{ \frac{\bar{h}^3(1+\alpha^3)}{\bar{h}^3 + \alpha^3} \right\} - \left\{ L - L_2 + 2\sqrt{3}\,(T - T_2) \right\} \right], \quad (26)$$

where

$$L = \ln \left[\frac{(\bar{h} + \alpha)^2}{\bar{h}^2 - \alpha\bar{h} + \alpha^2} \right], \quad T = \tan^{-1}\left(\frac{2\bar{h} - \alpha}{\alpha\sqrt{3}} \right)$$

and L_1, L_2 and T_1, T_2 are their values when $\bar{h} = a$ and $\bar{h} = 1$ respectively.

Also

$$\bar{h}_0 = \frac{\alpha}{2} \left[L_1 - L_2 + 2\sqrt{3}(T_1 - T_2) \right] / \ln \left\{ \frac{a^3(1+\alpha^3)}{a^3 + \alpha^3} \right\}. \quad (27)$$

The dimensionless load capacity is obtained as

$$\bar{W} = \frac{h_1^2 \, W}{\mu \overline{U} A^2 B} = - \frac{6}{(\ln a)^2} \int_a^1 \frac{(\bar{h} - \bar{h}_0)\ln \bar{h}}{\bar{h}\,(\bar{h}^3 + \alpha^3)} \, d\bar{h} \quad (28)$$

The dimensionless friction is given by

$$\bar{F} = \frac{h_1 F}{\mu U AB} = \frac{1}{4\alpha \ln a} \left[4\alpha \left(1 - \frac{1}{a}\right) \right.$$

$$\left. - \frac{\left\{L_1 - L_2 + 2\sqrt{3}(T_1 - T_2)\right\}^2}{\ln \left\{\frac{a^3(1+\alpha^3)}{a^3 + \alpha^3}\right\}} - 2\left\{L_1 - L_2 + 2\sqrt{3}(T_2 - T_1)\right\} \right] \qquad (29)$$

The dimensionless centre of pressure is obtained as

$$\frac{\bar{\bar{x}}}{A} = \frac{3}{\bar{W}(\ln a)^3} \int_a^1 \frac{(\bar{h} - \bar{h}_0)(\ln \bar{h})^2}{\bar{h}(\bar{h}^3 + \alpha^3)} \, d\bar{h} + 1. \qquad (30)$$

2.2.3 Results and discussion

The numerical results for dimensionless load capacity, centre of pressure and friction are shown in Tables 4 to 6.

The extent of the effect of porosity is determined by the additional paramter $\psi = kH/h_1^3 = \alpha^3/12$ which appears as a consequence of the introduction of porous facing.

It is seen from Table 4 that, for values
of $\psi \geq$ 0.01, load is decreased significantly as
compared to that of a solid bearing. For each ψ there
is an optimum value of a for which the load is
maximum.

Table 5 shows that the centre of pressure
Is moved closer to the inlet face when a or ψ
increases.

It is seen from table 6 that the dimension-
less friction $\bar{F}$ is decreased significantly for
values of $\psi \geq$ 0.01. The same thing happens for larger
values of a.

All the tables 4 to 6 show that, for
$\psi \leq$ 0.001, a porous slider behaves like an impermeable
one. So, for these values of ψ , the self-lubricating
nature of a porous bearing is maintained without
significantly affecting the other bearing characteristics.

TABLE 4

Values of dimensionless load $\bar{W}$ for various values of ψ and a.

a \ ψ	0.0001	0.001	0.01	0.1
2	0.1414	0.1410	0.1372	0.1124
3	0.1502	0.1498	0.1461	0.1201
4	0.1372	0.1369	0.1338	0.1113

TABLE 5

Values of dimensionless centre of pressure $\bar{x}/A$ for various values of ψ and a.

a \ ψ	0.0001	0.001	0.01	0.1
2	0.7937	0.7935	0.7916	0.7760
3	0.5204	0.5199	0.5154	0.4755
4	0.2799	0.2791	0.2724	0.2118

TABLE 6

Values of dimensionless friction $\bar{F}$ for various values of ψ and a.

a \ ψ	0.0001	0.001	0.01	0.1
2	0.7985	0.7982	0.7950	0.7745
3	0.7468	0.7464	0.7424	0.7152
4	0.7148	0.7144	0.7104	0.6827

2.3 SQUEEZE FILM BETWEEN CURVED CIRCULAR PLATES

A squeeze film is a very thin fluid layer between two surfaces which are parts of a machine, having normal relative motion and thus approaching each other. The relative normal motion of the surfaces causes the fluid to flow towards less constrained boundaries, resulting in the development of high pressures which in turn support the load and hence keep off the approaching surfaces from potential contact. This fact is used in frictional devices such as clutch plates in automotive transmissions etc.

Wu [17] analysed the squeeze film behaviour between two annular disks when one of them had a porous facing. The load capacity and the response time were decreased due to the introduction of the porous facing. Later, many investigators [18, 22, 10] considered similar problems for rectangular, circular and various geometries. All the above investigators assumed that the plates were flat.

Recently Murti [43] introduced a new exponential function to describe the curved film

between two circular plates. The exponential function
not only simplified the analysis but also helped in
obtaining the response time of squeeze films by avoiding
complicated numerical integration. He claimed that his
results could be usefully exploited in predicting squeeze
film behaviour in machine elements like gears and
cylindrical rollers.

While the above analysis considered the
two circular plates to be impermeable, in this section
we assume that the upper plate is porous.

2.3.1 Mathematical formulation

The configuration consists of two plates,
each of radius r_1. The upper plate is curved and has
a porous facing of thickness H which is backed by a
solid wall (Fig. 6). The lower plate is fixed and flat.
The film thickness, as in $[43]$, is taken as

$$h = \alpha_0 \, e^{-\beta r^2} , \qquad (31)$$

where α_0 is the central film thickness and β is
the curvature of the upper plate.

$$h = \alpha_0 e^{\beta r^2}$$

$\beta < 0$

POROUS FACING
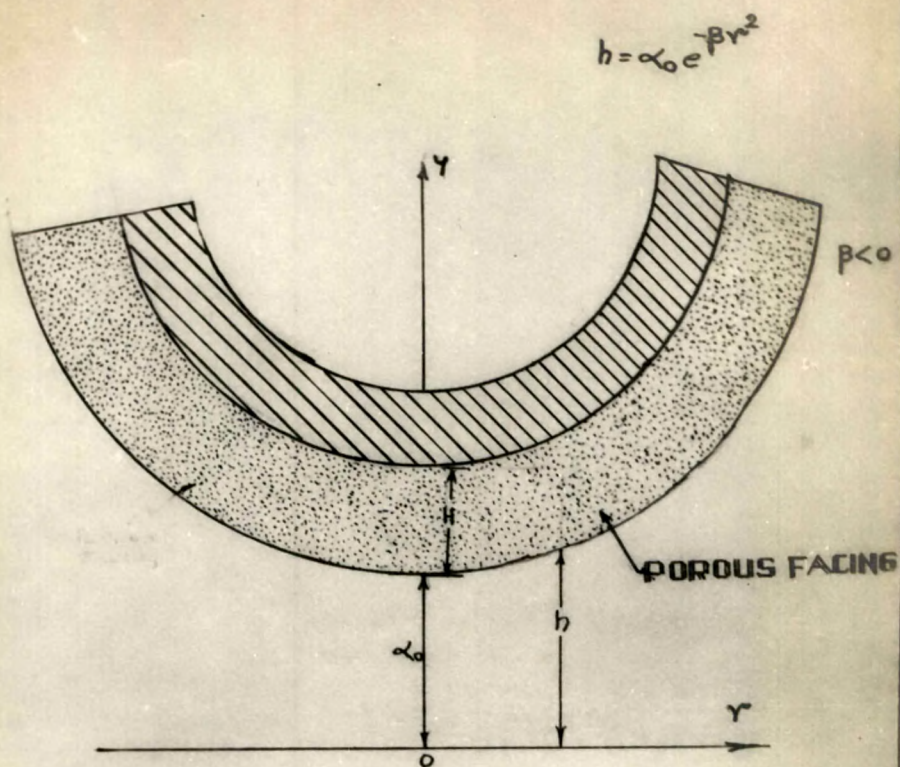
FIG. 6. SQUEEZE FILM BETWEEN POROUS CURVED CIRCULAR PLATES.

In dimensionless form it is

$$\frac{h}{\alpha_0} = e^{-\bar{\beta}R^2},$$ (32)

where

$$R = \frac{r}{r_1} \quad \text{and} \quad \bar{\beta} = r_1^2 \beta$$ (33)

The upper plate moves normal to itself approaching the lower plate with uniform velocity $\dot{\alpha}_0$. The modified Reynolds equation governing the system is

$$\frac{1}{r} \frac{d}{dr} (rh^3 \frac{dp}{dr}) = 12 \mu \left[\dot{\alpha}_0 - \frac{k}{\mu} (\frac{\partial P}{\partial y})_{y=h} \right],$$ (34)

where P is the pressure in the porous region satisfying the equation

$$\frac{1}{r} \frac{\partial}{\partial r} (r \frac{\partial P}{\partial r}) + \frac{\partial^2 P}{\partial y^2} = 0.$$ (35)

The equations (34) and (35) are coupled. Using Morgan-Cameron approximation, they are uncoupled as in [10] and we accordingly have

$$\frac{1}{r} \frac{d}{dr} \left[r \left(h^3 + 12kH \right) \frac{dp}{dr} \right] = 12 \mu \, \dot{\alpha}_0 \qquad (36)$$

2.3.2 Solutions

Substituting equation (31) into equation (36) and then solving it under the boundary conditions

$$\frac{dp}{dr} = 0 \quad \text{when} \quad r = 0 \quad \text{and} \quad p = 0 \quad \text{when} \quad r = r_1 \qquad (37)$$

the dimensionless pressure is

$$\bar{p} = - \frac{\alpha_0^3 \, p}{\mu \, r_1^2 \, \dot{\alpha}_0} = - \frac{1}{12 \psi \bar{\beta}} \, \ln \left(\frac{1 + 12 \psi \, e^{3\bar{\beta}R^2}}{1 + 12 \psi \, e^{3\bar{\beta}}} \right) \qquad (38)$$

where

$$\psi = \frac{kH}{\alpha_0^3}$$

The dimensionless load capacity is

$$\bar{W} = \frac{\alpha_0^3 \, W}{2\pi \, \mu \, r_1^4 \, |\dot{\alpha}_0|} = \frac{1}{12 \psi \bar{\beta}} \int_0^1 R \ln \left(\frac{1 + 12 \psi \, e^{3\bar{\beta}}}{1 + 12 \psi e^{3\bar{\beta}R^2}} \right) dR \qquad (39)$$

The time taken for reduction in central film thickness from α_{01} to α_{02} is

$$\Delta t = \frac{2\pi \, \mu \, r_1^4}{\overline{W}} \, \frac{1}{2} \, (\, \frac{1}{\alpha_{02}^2} - \frac{1}{\alpha_{01}^2} \,) \, \overline{\overline{W}} \qquad (40)$$

2.3.3 Results and discussion

By making $\psi \to 0$ in equations (38) – (40), the equations agree with those obtained by Murti [43] in the non-porous case.

The load capacity given by equation (39) is computed by Simpson's one-third rule after dividing the interval of integration into one hundred equal parts and is presented in tabular form.

Tables 7 and 8 show that the load capacity decreases when the permeability paramter ψ increases in both the cases of convex and concave pads. They confirm the observations by Murti [43] that the load capacity sharply rises with the curvature parameter $\overline{\beta}$ in the case of concave pads.

Using the values of $\overline{W}$ given in Tables 7 and
8 in equation (40) the time required to attain a
specified central film thickness can be calculated very
easily.

TABLE 7

Values of dimensionless load capacity $\overline{W}$ in the case
of convex ($\overline{\beta} < 0$) pads for various values of $\overline{\beta}$ and ψ.

$\overline{\beta}$ \ ψ	0.0001	0.0010	0.1000	1.0000
-0.4	0.3512	0.3493	0.2205	0.0525
-0.6	0.2486	0.2475	0.1707	0.0484
-0.8	0.1800	0.1794	0.1309	0.0434
-1.0	0.1334	0.1330	0.1006	0.0378
-5.0	0.0067	0.0066	0.0053	0.0026

TABLE 8

Values of dimensionless load capacity $\bar{W}$ in the case of concave ($\bar{\beta} > 0$) pads for various values of $\bar{\beta}$ and ψ .

$\bar{\beta}$ \ ψ	0.0001	0.0010	0.1000	1.0000
0.4	1.728	1.684	0.453	0.060
0.6	2.690	2.577	0.494	0.061
0.8	4.243	3.949	0.526	0.061
1.0	6.763	5.999	0.550	0.062
5.0	490.248	56.159	0.621	0.063